Global Optimization of H-Passivated Si Clusters at the Ab Initio Level via the GAM1 Semiempirical Method

Yingbin Ge and John D. Head*

Department of Chemistry, University of Hawaii, 2545 The Mall, Honolulu, Hawaii 96822

Received: January 5, 2004; In Final Form: March 5, 2004

A genetic algorithm (GA)-based procedure for finding the global minimum of medium-sized Si_xH_y clusters at the ab initio level is presented. Semiempirical calculations are used to prescreen the relative energies of the many locally optimized Si_xH_y structures generated by the GA. The AM1 semiempirical method used in our original global optimization strategy produces cluster energies appreciably different from the ab initio ranking. To improve the AM1 energy ranking we recently explored using for each specific Si_xH_y stoichiometry two coupled GAs: (1) a parametrization GA (PGA) for finding better semiempirical GAM1 parameters for Si and (2) a cluster global optimization GA (CGA) that uses the GAM1 parameters in the cluster energy prescreening. The two GAs method is a more reliable approach for global optimization of different Si_xH_y stoichiometries because the GAM1 parameters adjust to whether the Si atoms are partially or completely passivated by H atoms. Unfortunately, even for medium-sized Si_xH_y clusters we find the two GAs method is too computationally demanding. In this paper we examine under what conditions the GAM1 parameters obtained for a specific small Si_xH_y stoichiometry could be successfully transferred to larger clusters so that only the CGA global search need be performed. We choose Si_7H_{14} as the starting stoichiometry since it can adopt various possible structures which model a Si_7 core completely passivated by H atoms. We find the resulting GAM1 parameters obtained from the Si_7H_{14} training set produce relative cluster energies matching well with the ab initio energy rankings for larger Si_xH_y clusters which also have complete H atom passivation. Whereas for the low H-passivated Si_xH_y clusters, the GAM1 energy rankings are no better than the previous AM1 results. We use Si_7H_{14} GAM1 parameters to repeat our search for the $Si_{10}H_{16}$ and $Si_{14}H_{20}$ global minima. Unlike the AM1 method, now both GAM1 and MP2 ab initio calculations give the lowest energy for the cluster with a completely passivated diamond-like Si core structure. The Si_7H_{14} GAM1 parameters not only improve our confidence that we are finding the true global minima but also reinforce our earlier conclusion that $Si_{10}H_{16}$ and $Si_{14}H_{20}$ are at their preferred level of H passivation. We illustrate the range of applicability of the Si_7H_{14} GAM1 parameters by determining the global minima for $Si_{10}H_{14}$ and $Si_{14}H_{18}$ stoichiometries. The global minima for these two later clusters demonstrate why global optimization methods are useful since their structures cannot be easily obtained by local optimization calculations initiated by simply removing two H atoms from the $Si_{10}H_{16}$ and $Si_{14}H_{20}$ global minima.

1. Introduction

Nanometer-sized Si particles have potentially interesting optoelectronic properties which could be useful in various technological applications. Since Si only clusters are highly unstable due to dangling bonds on the surface Si atoms a practical device will most likely be fabricated from silicon clusters whose surfaces are passivated by some chemically inert ligand. For these reasons we have been investigating the structures of Si_xH_y clusters where the H atoms serve as a prototypical passivating ligand. Several other groups have also been theoretically and/or experimentally exploring the possible structures for small- to medium-sized silicon hydride clusters.[1−11] Not only is finding the Si_xH_y global minimum structure important, but we also determine how many H atoms are actually needed to completely passivate the Si_x core. We applied a genetic algorithm (GA)[12−15] to find the cluster with the global minimum energy at the ab initio level for a particular Si_xH_y stoichiometry.[16] We used the AM1 semiempirical method[17] as a fast computational procedure to screen the energies for the many different Si_xH_y clusters generated during the GA and then searched among the low AM1 energy structures for the one with lowest ab initio energy. Our search strategy starts from a set of random Si_xH_y structures and avoids the explicit introduction of structures which might be expected from chemical intuition to have low energy. When the Si_x core is over passivated the method automatically produces Si_xH_{y-2} and H_2 structures. Our calculations confirmed the chemically expected result that the Si cores of the small- to medium-sized Si_xH_y clusters favor forming diamond-lattice-like structures provided they are surrounded with enough passivating ligands.[16] We have proposed that the Si_{10} and Si_{14} clusters need 16 and 20 H atoms to be fully passivated so as to eliminate any dangling bonds on the Si surface and avoid forming structures containing small and strained three- or four-membered Si rings. Unfortunately the energy ranking determined by the original AM1 method differed appreciably from the ab initio energy ranking. Even for well-passivated Si_xH_y clusters, the ab initio global minimum is often not the AM1 global minimum, where we designate the ab initio global minimum to mean the lowest energy isomer that has been

* Address correspondence to this author. Phone: 808-956-5787. Fax: 808-956-5908. E-mail: johnh@hawaii.edu.

10.1021/jp049949o CCC: $27.50
Published on Web 04/14/2004

found so far by any method at the ab initio level. For instance, previously we found nine $Si_{10}H_{16}$ structures with AM1 energies lower than the cluster with a diamond-lattice-like Si_{10} core corresponding to the ab initio global minimum.[16] To guarantee finding the true ab initio global minimum for the $Si_{10}H_y$ clusters, we had to examine up to 20 of the lowest AM1 energy clusters at the ab initio level. However, this strategy still failed when we attempted to find the global minimum of $Si_{14}H_{20}$ at the ab initio level. Since the number of local minima increases exponentially,[18] while the total energy scales only linearly, with the size of the cluster, we estimate that the larger Si_xH_y clusters will have an exponentially increased number of local minima residing in a very narrow energy range. A few kilocalories per mole relative energy deviation between the AM1 method and the ab initio method could easily lead to totally different energy rankings and explains why the true ab initio global minimum of the larger $Si_{14}H_{20}$ clusters was not found among the 20 clusters with lowest AM1 energies.[16] We identified the true ab initio $Si_{14}H_{20}$ global minimum by considering Si core fragments with a diamond-lattice-like structure.

To improve our reliability at finding the ab initio global minimum for a Si_xH_y cluster we developed a second global optimization strategy that utilizes two coupled genetic algorithms.[19] One of the GAs (the PGA) is used to reoptimize the AM1 parameters for Si[22] based on an iteratively augmented training set of Si_xH_y clusters treated at the ab initio level, and the other GA (the CGA) is essentially our original GA[16] used to search for the cluster ab initio global minimum but now using the reoptimized AM1 parameters for Si. The usual philosophy with a semiempirical method is to find a set of parameters which are applicable to a wide range of chemical environments. The goal of the GA optimized AM1 (GAM1) parameters is to have parameters which more accurately predict the energy but for a narrower range of chemical systems. In our studies on Si_6H_2 and Si_6H_6 clusters the GAM1 parameters significantly improved the semiempirical energy ranking of the different structures for a specific stoichiometry.[19] For instance, the final Si_6H_2 GAM1 parameters enabled the CGA to find the same global minimum structure at both the ab initio and semiempirical levels, whereas the Si_6H_6 GAM1 parameters resulted in the CGA finding three nearby low-energy local minima having the same Si framework as the Si_6H_6 ab initio global minimum. Since the GAM1 parameters for Si automatically adjust to different extents of H-passivation we feel this approach improves our ability at ultimately finding the ab initio global minimum for Si_xH_y clusters with various stoichiometries. Hartke has used a similar approach in the global optimization of small Si only clusters where a Si empirical potential is parametrized against the true cluster energy calculated by some ab initio method.[20,21] Unfortunately, the GAM1 reparametrization work means that the coupled GA method is not very efficient when we try to globally optimize larger clusters such as the well-passivated $Si_{10}H_{16}$ cluster. In this paper we explore how transferable the GAM1 parameters obtained from a Si_7H_{14} training set are to larger clusters with comparable levels of passivation. We choose Si_7H_{14} since it can form a series of structures close in energy which are representative of the Si core being completely H-passivated. Clearly, if the Si_7H_{14} GAM1 parameters produce a ranking matching the ab initio calculations on larger clusters we can then reliably use the much faster single GA approach to identify the global minimum for these larger clusters.

The remainder of the paper is organized as follows. Details on the computational methods are presented in the next section. We describe the two genetic algorithms used for finding (1) the optimum semiempirical parameters (PGA) and (2) the cluster global minimum (CGA). We also describe how the semiempirical and ab initio calculations are performed. The results and discussion are presented in the third section. This section starts by describing the results from the GAM1 parametrization with the Si_7H_{14} training set and the PGA. We then explore the transferability of Si_7H_{14} GAM1 parameters to larger Si_xH_y clusters having different levels of H-passivation. The final part of the Results and Discussion section demonstrates the range of application of the GAM1 parameters in the global optimization of the $Si_{10}H_{16}$, $Si_{10}H_{14}$, $Si_{14}H_{20}$, and $Si_{14}H_{20}$ clusters. Our results show for the clusters with high levels of H-passivation that the Si_7H_{14} GAM1 parameters outperform the AM1 method by better matching with the MP2 relative energies. Both the GAM1 and MP2 calculations consistently rank the diamond-lattice-like structures of $Si_{10}H_{16}$ and $Si_{14}H_{20}$ as the most stable isomers. Concluding remarks are given in the final section of this paper.

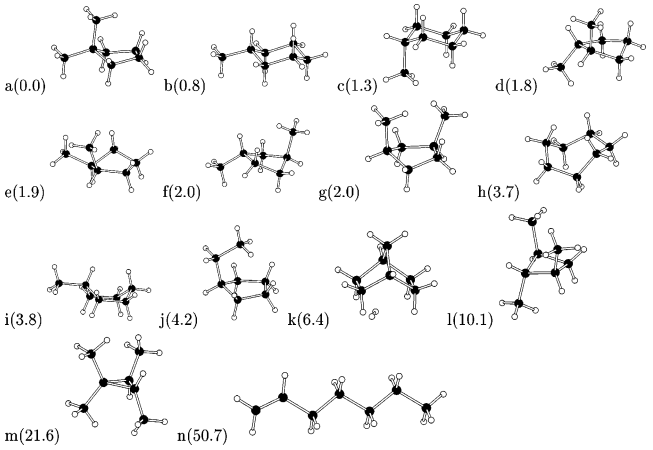

Figure 1. The MP2/6-31G* locally optimized geometries for the Si_7H_{14} training set. The MP2 relative energies are given in parentheses in kcal/mol.

2. Computational Methods

2.1. Parametrization Genetic Algorithm (PGA). The main goal of this paper is to find the correct global minimum of various well-passivated Si_xH_y clusters at the MP2[24] level. We start by selecting a training set consisting of relatively small Si_7H_{14} clusters as being suitable for reparametrizing the AM1 method. Si_7H_{14} is large enough that it can adopt various configurations, ranging from linear structures through three- to seven-membered-ring structures, which represent common partial structures found in a well-passivated Si_xH_y cluster. The 14 different MP2 optimized Si_7H_{14} structures selected to be in the training set are shown in Figure 1 along with their corresponding MP2 energies computed with a 6-31G* basis set[25,26] listed in parentheses. We include low-energy and some high-energy structures in the training set to ensure that both low- and high-energy structural features are reasonably modeled by the GAM1 parameters. In our previous work on the Si_6H_2 and Si_6H_6 stoichiometries we found a cluster global optimization (CGA) run with the new GAM1 parameters a useful check that we have sufficient low-energy structures in the training set.[19]

The semiempirical calculations are all performed with the original AM1 equations. We only reoptimize the 16 Si atom parameters: the atomic core integrals U_{ss} and U_{pp}, the Slater type orbital exponents ζ_s and ζ_p, the resonances β_s and β_p, the core−core repulsion term α, and the 9 core repulsion function parameters (K_{1-3}, L_{1-3}, and M_{1-3}).[22] In our previous paper, we

simply changed the values of the above 16 AM1 parameters in the data block of mpcdat.src in the GAMESS package and did not correctly take into account changes needed for the one-center two-electron integral terms.[19] In the present work we now correctly compute the one center two electron integral terms: fortunately we find our previous GAM1 parameters[19] are not significantly affected by the small errors present in the one center terms.

The PGA is only slightly modified from our earlier work.[19] We still use a population size of 100 since we find this balances the efficiency and effectiveness of the parameter global optimization. The initial 100 sets of different GAM1 parameters are randomly assigned real number values with a smaller range of ±3% from the original AM1 parameters. After the initial 100 fitness values are obtained, the top 10% GAM1 parameter sets with the smallest fitness values are copied directly into the offspring generation. The top 30% (including the top 10 mentioned above) are put into the breeding pool with equal weight, while the least fit 70% are eliminated from the generation. Pairs of parents are randomly chosen from the breeding pool to perform the uniform crossover to generate the remaining 90% offspring. Each gene of an offspring has a 50%−50% chance of inheriting the gene of one of the two parents at the same position. The mutation amplitude is also reduced to 2% since we find small modification of the original AM1 parameters is good enough for matching relative energies of well-passivated Si_xH_y clusters calculated by the semiempirical and the ab initio methods. We also want to avoid dramatic change of the AM1 parameters when using this relatively smaller Si_7H_{14} training set.

The GAM1 parameters are found by minimizing a fitness function f consisting of an energy and a gradient part:

$$f = f_E + f_G \tag{1}$$

For each distinct parameter set a GAM1 single-point energy is evaluated for every geometry in the training set. We define the energy-related fitness function f_E to be the root-mean-square (rms) deviation between the GAM1 and MP2 single-point energies times a penalty coefficient P:

$$f_E = P[\sum_{i=1}^{N_c}(E_i^{GAM1} - E_i^{MP2} + D)^2/N_c]^{1/2} \tag{2}$$

where D is the difference between the MP2 and GAM1 average energies for the training compounds and is introduced to maximize the coincidence of the GAM1 and MP2 relative energies:

$$D = \sum_{i=1}^{N_c}(E_i^{MP2} - E_i^{GAM1})/N_c \tag{3}$$

Since it is possible that some of the trial GAM1 parameters cause poor SCF convergence, we evaluate the fitness function using only the N_c training compounds which are SCF converged. The penalty coefficient P is designed to increase when one or more SCF calculations fail to converge:

$$P = e^{2.0(N_T - N_c)/N_T} \tag{4}$$

where $N_T(=14)$ is the total number of compounds in the training set. The gradient-related fitness value is determined from root mean square of the squared GAM1 energy gradient, G_i^{GAM1}, evaluated at the MP2 optimized geometry for structure i in the training set:

$$f_G = P[\sum_{i=1}^{N_c}(G_i^{GAM1})^4/N_c]^{1/2} \tag{5}$$

Rossi and Truhlar used a GA to obtain specific reaction parameters for use in dynamics calculations on the $Cl + CH_4 \rightarrow HCl + CH_3$ reaction.[27] They also used a fitness function that included both an energy and a gradient term. However, our experience suggests that the decrease in the deviation of energy after the GAM1 optimization is roughly proportional to the square of the GAM1 root-mean-square gradient when starting from a MP2 optimized geometry. We find including the higher fourth power on the gradient term is more effective at reducing differences between the GAM1 and the MP2 optimized geometries. We did not include the gradient term in the fitness function in our previous paper[19] since we found that the geometry and energy of the low H-passivated Si_xH_y clusters could change dramatically during local optimization even when the starting geometry had a small gradient.

2.2. Cluster Genetic Algorithm (CGA). We have slightly modified the previous genetic algorithm used for globally optimizing the Si_xH_y clusters[16] to facilitate more efficient calculations in a multiprocessor computing environment. The global optimization starts from N initial random structures of the Si_xH_y clusters as our ancestor population, where N is the population size that depends on the size of the molecule. In this paper we use a population size of 60 for $Si_{10}H_y$ stoichiometries and 120 for the larger $Si_{14}H_y$ ones. The fitness value f_i of the ith initial individual cluster is taken as the absolute value of the GAM1 energy of the locally optimized cluster. The lower the energy of an individual, the higher is its fitness. Tournament selection instead of Boltzmann selection is used to select random parent couples which mate to produce offspring with guaranteed variety for the next generation. Each parent used for the mating process is chosen by first randomly selecting eight individual clusters from the current population and the one with lowest energy is then taken as one parent. To run our cluster global optimization on a multiprocessor environment more efficiently, we reorganized our CGA source code so that it no longer explicitly treats separate generations. Previously we only started work on a new generation after all individuals in the previous generation have been locally optimized: the new strategy now performs parent selection, mating process, and local optimization for a new individual as soon as any cluster local optimization job is finished on a processor. This new strategy reduces the wall clock time since it avoids processors being idle while waiting for other local optimization jobs in the same generation to be completed.

Generally we want the mating methods to keep the good features of the better (lower energy) parents while some mutations are performed to help maintain the variety of the population. Three mating methods are adopted. One is to take the arithmetic mean of the Cartesian coordinates from two parent geometries. The second method is to take a fragment of Si atoms from one parent and replace it with the fragment of the other parent with the same number of atoms, and also cut a fragment of H atoms from one parent and replace it with a fragment of H atoms in the other parent with the same number of atoms. The last method is to cut each parent into halves and then recombine one-half from each parent to generate the offspring. The first and second mating processes produce drastic mutations, while the third method retains much of the local structures of

both parents. The probabilities used for selecting the first, second, and third methods are 25%, 25%, and 50%, respectively. After the mating process, an offspring is generated and fully optimized again by the GAM1 method. To avoid same structures occupying the population repeatedly, we replace the least stable structure of the current population with a new offspring only if this offspring has lower energy and is not identical with any individual in the current population. We have developed an efficient and effective strategy to determine whether the offspring generated is identical with any cluster already present in the current population. We simply compare the energy and principal moments of inertia of new offspring with the values for every individual in the current population. We assume that the new offspring is identical with a previous individual when their energies differ by less than 10^{-3} au and their three principal moments of inertia all agree within 1%. Our experience shows this threshold is tight enough to keep distinct offspring clusters while not too tight to have many essentially identical individuals occupying the population.

2.3. Semiempirical and ab Initio Methods. All of the semiempirical and ab initio calculations were performed with the GAMESS program.[23] The GAM1 parameters were introduced into the GAMESS program by modifying the appropriate Si atom AM1 parameters. Initially the CGA finds the many low-energy Si_xH_y clusters using the GAM1 method, then we determine the ab initio global minimum by locally optimizing the 20 lowest GAM1 energy structures with the MP2 method.[24] The ab initio calculations use a 6-31G* basis for the clusters containing 10 or fewer Si atoms;[25,26] whereas the Hay−Wadt effective core potential (ECP) and valence basis set for Si[28] augmented with a d function[29] and the Dunning−Hay basis for H[30] were used to reduce the computational effort for the larger $Si_{14}H_{20}$ and $Si_{14}H_{18}$ clusters. Consistent with the work of others,[29,31] our tests show that the relative energies of the well-passivated Si clusters calculated by the MP2 method match well with the much more expensive methods which include higher levels of electron correlation such as MP4 and CCSD(T). We also performed some vibrational frequency calculations to estimate zero-point energy (ZPE) corrections and Gibbs free energies using HF/6-31G* calculations for $Si_{10}H_{16}$ and $Si_{10}H_{14}$ and HF/3-21G calculations for the larger $Si_{14}H_{20}$ and $Si_{14}H_{18}$ clusters. All of the frequencies were scaled with Scott and Radom correction factors.[32]

3. Results and Discussion

3.1. GAM1 Parameter Global Optimization with the Si_7H_{14} Training Set. The Si_7H_{14} training set and the relative MP2 energies for the locally optimized structures are shown in Figure 1. Both the AM1 and the new GAM1 parameters obtained from the Si_7H_{14} training set are listed in Table 1. The original AM1 parameters for the Si atom were obtained from a wide variety of compounds containing one or more Si atoms[22] and consequently it should not be surprising that different GAM1 parameters are obtained when treating a narrower range of compound types. On the other hand, we should not anticipate major changes in the parameters since the AM1 method has generally been found to give reasonable relative energies for Si-containing compounds.[22] The most significant changes occur for the ζ_s and β_s parameters which are reduced by 18% and 12%, respectively, while the rest of the GAM1 parameters from the Si_7H_{14} training set differ by less than 10% from the corresponding AM1 parameter. Previously the GAM1 parameters obtained with the Si_6H_2 and Si_6H_6 training sets showed greater differences from the original AM1 parameters presumably because of the presence of a greater fraction of low-coordinate Si atoms in these training sets.[19]

TABLE 1: Comparison of the AM1 Parameters and the Improved GAM1 Parameters Derived from a Si_7H_{14} Training Set

parameters	AM1	GAM1
U_{ss}/eV	−33.953622	−34.269578
U_{pp}/eV	−28.934749	−30.694633
ζ_s/au	1.830697	1.500623
ζ_p/au	1.284953	1.356890
β_s/eV	−3.784952	−3.321166
β_p/eV	−1.968123	−1.862159
α/Å^{-1}	2.257816	2.249007
K_1	0.250000	0.249818
K_2	0.061513	0.065260
K_3	0.020789	0.020458
L_1	9.000000	10.141849
L_2	5.000000	5.309296
L_3	5.000000	4.221081
M_1	0.911453	0.865394
M_2	1.995569	1.955345
M_3	2.990610	2.812023

TABLE 2: Comparison of the Si_7H_{14} Relative Energies for MP2 Optimized Geometries versus the AM1 and GAM1 Relative Energies Calculated at the MP2 Optimized Geometry (S.P.) and at the Optimized Semiempirical Geometry (Opt)

			AM1		GAM1	
structure	Si ring size	MP2	S.P.	Opt	S.P.	Opt
1(a)	5	0.0	0.0	−2.8	0.0	−0.3
1(b)	6	0.8	6.5	3.5	1.9	1.8
1(c)	6	1.3	6.1	3.4	1.8	1.7
1(d)	5	1.8	3.7	0.6	1.9	1.5
1(e)	5	1.9	3.7	0.5	1.9	1.4
1(f)	5	2.0	3.4	0.5	1.7	1.4
1(g)	5	2.0	3.2	0.4	1.5	1.1
1(h)	7	3.7	10.2	7.1	3.8	3.5
1(i)	6	3.8	6.3	3.5	2.5	2.2
1(j)	5	4.2	5.8	3.4	2.6	2.4
1(k)	5, 5	6.4	2.3	−2.0	5.9	4.4
1(l)	4	10.1	10.7	6.5	9.2	8.0
1(m)	3	21.6	18.9	15.1	20.8	19.5
1(n)		50.7	49.3	42.6	50.5	47.3
rms dev			2.9	3.5	0.7	1.1

[a] The root-mean-square (rms) deviation between the semiempirical and the MP2 energies is evaluated by using eq 2. All energies are in kcal/mol.

Table 2 compares the relative MP2 optimized energies against the AM1 and GAM1 relative energies for all of the Si_7H_{14} training compounds. Table 2 includes the single-point AM1 and GAM1 relative energies computed at the MP2 optimized geometries and the AM1 and GAM1 energies obtained by reoptimizing the MP2 structures with the semiempirical calculations. Structure **1(a)** containing a five-membered Si ring is found to be the global minimum for all three methods and we use the **1(a)** MP2 optimized geometry as the zero reference for each of the MP2, AM1, and GAM1 relative energies. Table 2 shows the Si_7H_{14} training set to contain six MP2 optimized structures within 2 kcal/mol of the global minimum. The GAM1 single-point calculations have the smallest root-mean-square deviation and do the best job at reproducing the small MP2 energy differences in Table 2. The GAM1 single-point calculations give a definite improvement over the AM1 single-point relative energies. Since in a CGA we would locally optimize various cluster structures with the semiempirical method first before performing an ab initio optimization, it is also important to notice in Table 2 that the GAM1 root-mean-square deviation

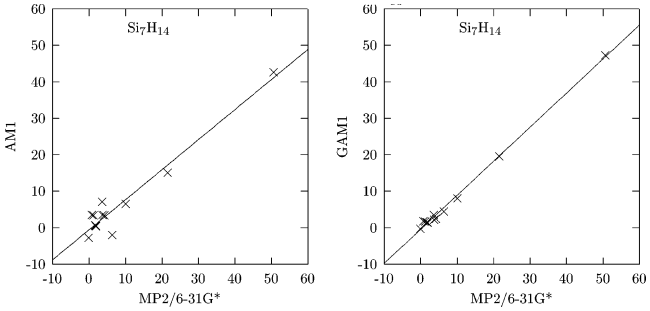

Figure 2. Comparison of the Si_7H_{14} AM1 (left) and GAM1 (right) relative optimized energies against MP2/6-31G* relative optimized energies. Energies are in kcal/mol.

increases slightly due to the small energy relaxation that occurs when each MP2 optimized structure is reoptimized with the GAM1 parameters. Nonetheless, the root-mean-square deviation for GAM1 optimized structures is still considerably better than the AM1 root-mean-square deviations. The small GAM1 energy relaxation after optimization is consistent with an improvement in the geometry capabilities, as well as providing more reliable energy rankings, for the GAM1 parameters obtained from using Si_7H_{14} training compounds. The average root-mean-square Cartesian energy gradients for stationary point structures (excluding **1(k)**) are 6.4×10^{-3} and 0.9×10^{-3} au for AM1 and GAM1, respectively. The **1(k)** stationary point structure has much larger root-mean-square AM1 and GAM1 gradients of 9.4×10^{-3} and 6.6×10^{-3} au due to large gradients on the isolated H_2 molecule which are independent of the Si atom parameters values. In Figure 2 the relative AM1 and GAM1 optimized structure energies are plotted against the corresponding MP2 energy and this provides another illustration that the resulting Si_7H_{14} GAM1 parameters do a better job at simulating the expensive MP2/6-31G* calculations than the AM1 method.

Except for structure **1(n)**, all the Si_7H_{14} training compounds shown in Figure 1 contain a Si atom ring structure with sizes between three and seven Si atoms. Table 2 lists the Si ring size for each training compound and we see at the MP2 level that the seven lowest energy structures which are within 2 kcal/mol of each other contain either a five- or a six-membered Si ring. The AM1 calculations in Table 2 consistently underestimate the stability of both six- and seven-membered-ring structures relative to the five-membered-ring structures. This AM1 trend is found for the two low-energy six-membered-ring structures **1(b)** and **1(c)** and for the slightly higher energy structures **1(h)** and **1(i)**. The new Si_7H_{14} GAM1 parameters are able to correct for this deficiency and better reproduce the ab initio relative energies for the six- and seven-membered-ring structures.

The bicyclic structure **1(k)** is an example of Si_7H_{14} automatically losing a H_2 molecule because of over passivation. Despite containing 2 five-membered Si rings, AM1 predicts a low relative energy for structure **1(k)**, which suggests the AM1 parameters favor forming more compact Si_xH_y structures. This result may explain why in our previous research work[16] we obtained many low relative energy structures with a H_2 molecule detached at the AM1 level which had appreciably higher relative energies at the ab initio level. The GAM1 method increases the single-point relative energy of **1(k)** to 5.9 kcal/mol although the energy of the optimized GAM1 structure still relaxes to 4.4 kcal/mol. Of the total energy change 1.4 kcal/mol is due to the H_2 relaxing from the optimized MP2 geometry to the equilibrium AM1 geometry as a result of the relatively large H_2 energy gradients described above for the **1(k)** single-point structure. Consequently, we expect the present GAM1 parameters should also give a better relative energy estimate when a H_2 molecule is lost from a Si_xH_y cluster.

3.2. Transferability of the Si_7H_{14} GAM1 Parameters. To test the transferability of the Si_7H_{14} GAM1 parameters to larger Si_xH_y clusters we have repeated the semiempirical local optimizations on all of the $Si_{10}H_y$, $y = 4$, 8, 12, 16, 20, and the $Si_{14}H_{20}$ cluster structures we obtained from our earlier cluster global optimization effort.[16] The $Si_{10}H_y$ and $Si_{14}H_{20}$ clusters contain Si atoms in a range of environments. Low passivation is exhibited for the clusters with the $Si_{10}H_4$ and $Si_{10}H_8$ stoichiometries since they all contain at least two Si radicals. Three of the $Si_{10}H_4$ structures we have obtained even contained two biradical Si atoms. The 10 low AM1 energy $Si_{10}H_{12}$ structures we found previously all have the Si atoms 4-fold coordinated, but these structures still have significant ring strain due to the presence of small three- or four-membered Si rings indicative of intermediate passivation. Each of the Si atoms in the different $Si_{10}H_{16}$, $Si_{10}H_{20}$, and $Si_{14}H_{20}$ clusters are essentially tetrahedrally coordinated with either other Si or H atoms and the Si_x core is well- or even over-passivated by H atoms. This last group of clusters does not contain any three- or four-membered Si atom rings, further suggesting that the Si cores of these clusters have a similar level of passivation as the low-energy Si_7H_{14} clusters. As expected we find the GAM1 method obtained by using the Si_7H_{14} training compounds dramatically outperforms the original AM1 method for $Si_{10}H_{16}$, $Si_{10}H_{20}$, and $Si_{14}H_{20}$ clusters. Figure 3 displays the typical energy-comparison charts for the under-passivated $Si_{10}H_8$ structures and for the two well-passivated stoichiometries $Si_{10}H_{16}$ and $Si_{14}H_{20}$. Figure 3 shows the general result that for well-passivated stoichiometries, such as $Si_{10}H_{16}$ and $Si_{14}H_{20}$, the GAM1 method produces local optimized relative energies which match well with the MP2 relative energies, whereas for the stoichiometries representative of a lower level of H passivation, such as $Si_{10}H_8$, the GAM1 parameters give results which are not any better than those obtained from the original AM1 parameters. Our earlier work[19] suggests that a different set of GAM1 parameters obtained from a training set built from Si clusters corresponding to a lower level of H-passivation is needed to better reproduce the MP2 energies for this stoichiometry. Finally, it is worth noting that the diamond-lattice-like $Si_{10}H_{16}$ and $Si_{14}H_{20}$ clusters, described in more detail below, both produce the lowest energies with the GAM1 and MP2 methods.

3.3. CGA-Only Global Optimization. In our previous paper we advocated the reoptimization of the AM1 parameters for each specific Si_xH_y stoichiometry.[19] Unfortunately, performing a global optimization with a coupled PGA and CGA soon becomes an expensive undertaking for large clusters such as $Si_{10}H_{16}$ and $Si_{14}H_{20}$. The results in the previous subsection suggest that the GAM1 parameters obtained for a certain level of H-passivation may be transferred to larger cluster with comparable levels of H-passivation. In this subsection we analyze whether the GAM1 parameters obtained from the Si_7H_{14} training set do enable a more reliable CGA-only search for the ab initio global minimum of $Si_{10}H_{16}$ and $Si_{14}H_{20}$ than when using the AM1 parameters. In addition, to get some feel for the range of applicability of the Si_7H_{14} GAM1 parameters we also use the CGA to find the global minimum for the $Si_{10}H_{14}$ and $Si_{14}H_{18}$ stoichiometries which correspond to slightly lower extents of H-passivation.

$Si_{10}H_{16}$. We have repeated the global optimization of $Si_{10}H_{16}$ using the CGA and the GAM1 parameters obtained from the Si_7H_{14} training set to see if we still arrive at the same results as before.[16] Figure 4 shows the 20 lowest energy $Si_{10}H_{16}$ cluster

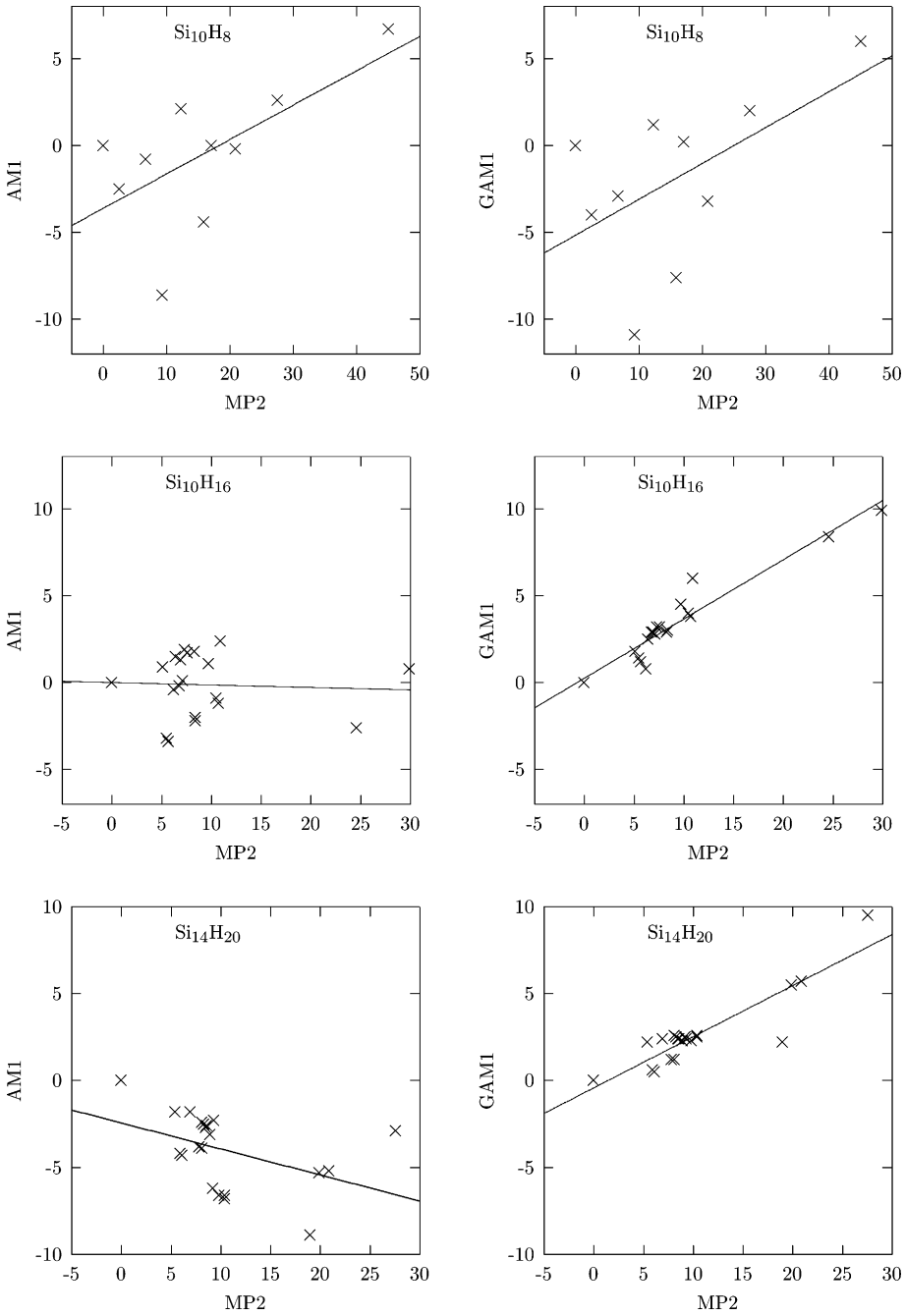

Figure 3. Comparison of AM1 and GAM1 relative optimized energies against MP2 relative optimized energies for representative stoichiometries $Si_{10}H_8$, $Si_{10}H_{16}$, and $Si_{14}H_{20}$. Energies are in kcal/mol.

structures listed in order of increasing MP2 energy found by the CGA. The global minimum **4(a)** has a diamond-lattice-like Si_{10} core structure. While the diamond-lattice structure is not unexpected, it is worth emphasizing that the CGA obtains this structure without any prior Si chemical bonding or structural bias being explicitly included in the algorithm. In our first CGA run, the global minimum structure **4(a)** was found after performing only 630 local GAM1 geometry optimizations. Nonetheless, to ensure that the **4(a)** structure is the true GAM1 global minimum, we kept the CGA running until 9000 local GAM1 geometry optimizations had been completed. We checked this result by running two other shorter CGA runs where only 3000 local geometry optimizations were performed but still found structure **4(a)** as having the lowest total energy. The structures shown in Figure 4 are the 20 distinct lowest GAM1 energy clusters found by the CGA which were subsequentially optimized at the MP2/6-31G* level. In the case of two enantiomers being located, we simply pick one of the structures to run the MP2 local optimization.

The Si_7H_{14} GAM1 parameters give the diamond lattice fragment $Si_{10}H_{16}$ as the lowest energy cluster, whereas in our earlier work the AM1 calculations ranked this structure as having the tenth lowest energy.[16] In addition, the GAM1 calculations now produce quite a number of other low-energy structures which are different from what were previously obtained.[16] We find the 20 lowest energy GAM1 structures to produce a 10.2 kcal/mol energy range at the MP2/6-31G* level compared with the previous 20 lowest AM1 structures which spanned a 23.5 kcal/mol MP2/lanl2dz(d) energy range. The AM1 calculations also produced two structures (3rd and 12th lowest energy) consisting of $Si_{10}H_{14}$ and H_2 which we used earlier to suggest that $Si_{10}H_{16}$ may be over-H-passivated.[16] Now, none of the present 20 low-energy GAM1 structures shown in Figure 4 have a H_2 dissociating from the $Si_{10}H_{16}$ nor do we find any structures

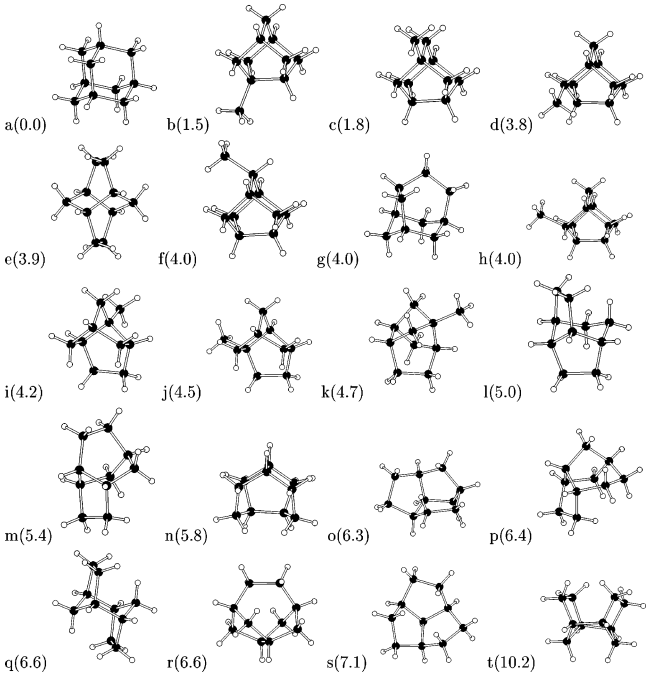

Figure 4. MP2/6-31G* optimized $Si_{10}H_{16}$ structures.

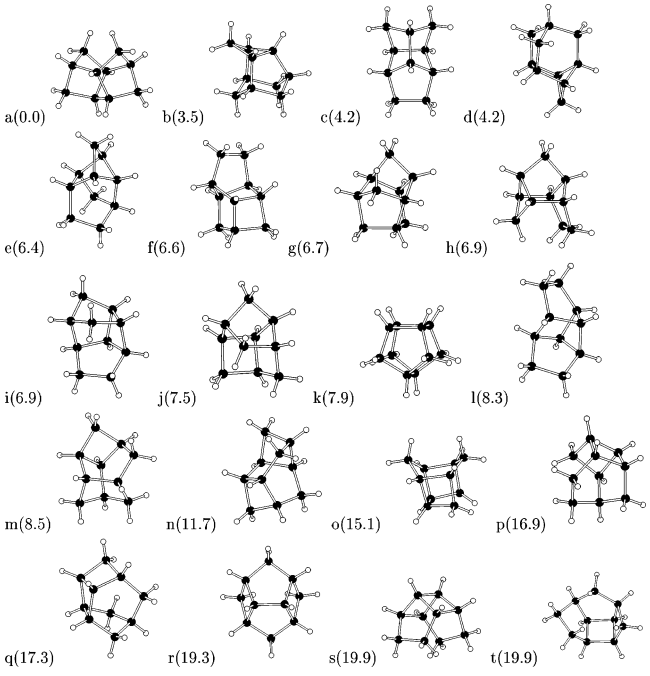

Figure 5. MP2/6-31G* optimized $Si_{10}H_{14}$ structures and their corresponding relative energies. The MP2 relative energies are given in parentheses in kcal/mol.

to contain high-energy three- or four-membered Si rings. The GAM1 and MP2 methods both rank the diamond-lattice-like structure **4(a)** as the global minimum while the AM1 method ranked structures **4(b)** and **4(c)** 3−4 kcal/mol below the diamond-lattice-like structure **4(a)**. The five low-energy structures **4(b−d)**, **4(f)**, and **4(h)** have basically the same Si core framework but with a silyl group at different positions. Their Si frameworks differ from the diamond-lattice-like structure **4-(a)** by forming a five-membered ring after removing a SiH_2 from one of the six-membered Si rings. Structure **4(e)**, like **4-(a)**, also consists of 4 six-membered Si rings but with an arrangement unrelated to the diamond lattice, whereas **4(g)** can be derived from **4(a)** by shifting a SiH_2 from one of the six-membered Si rings to another ring to produce a five- and a seven-membered Si ring. The narrow MP2 relative energy range for structures **4(a)** to **4(h)** illustrates that the energy cost of interconverting the diamond-lattice-like structure of **4(a)** to a related distorted structure can be very small. Some insight into why AM1 does not give **4(a)** as its global minimum is indicated by the results in Table 2 which show the AM1 energy for six-membered Si rings may be as much as 3 kcal/mol too high. In general we find the Si_7H_{14} GAM1 parameters to yield locally optimized $Si_{10}H_{16}$ structures which are very close to the final MP2 optimized structures, whereas the AM1 optimized structures tend to exhibit much larger geometry differences from the ab initio structures. We have also checked that the $Si_{10}H_{16}$ cluster energy rankings are not affected by the inclusion of zero-point energy (ZPE) corrections. The vibrational frequency calculations show the ZPE to vary by less than 0.4 kcal/mol between the 20 different $Si_{10}H_{16}$ structures.

To summarize, by performing a CGA using the GAM1 parameters obtained from the Si_7H_{14} training set and then computing the locally optimized geometries of the resulting low-energy $Si_{10}H_{16}$ structures we obtain stronger evidence supporting our previous proposal that the small- to medium-sized Si_xH_y clusters prefer to adopt diamond-lattice-like structures.[16] In addition we find no low-energy structures where the $Si_{10}H_{16}$ loses a H_2 molecule in agreement with our earlier work that this stoichiometry is the preferred level of complete H-passivation for the Si_{10} core.[16]

$Si_{10}H_{14}$. To test the range of applicability for the GAM1 parameters from the Si_7H_{14} training set we have searched for the global minimum of the $Si_{10}H_{14}$ stoichiometry. Three independent CGA runs were performed. In one run 9000 local geometry optimizations were performed while the two other shorter runs used only 3000 local geometry optimizations simply to check whether the same global minimum was located by the multiple runs. They all find the global minimum structure **5(a)** within 780, 600, and 300 local geometry optimizations, respectively. The geometries of the 20 lowest GAM1 energy structures were further optimized by using the MP2/6-31G* method and the resulting structures are shown in Figure 5 in the order of their MP2 relative energies. Our calculations find the GAM1 energy ranking for the different $Si_{10}H_{14}$ clusters still agrees well with the MP2 relative energies. Both the GAM1 and MP2 methods give structure **5(a)** as the global minimum. Thus, even for Si_xH_y stoichiometries which have slightly lower levels of H-passivation, we feel the GAM1 parameters still provide a reasonable energy ranking.

The relative energy range for the lowest 20 $Si_{10}H_{14}$ structures shown in Figure 5 is about 20 kcal/mol at the MP2 level. Thus, $Si_{10}H_{14}$ has a smaller number of low-energy isomers than we found for the $Si_{10}H_{16}$ stoichiometry. We think this is because the $Si_{10}H_{14}$ structures are more compact and they do not form several structures close in relative energy where a silyl group is just bound at different locations on the same Si_9 core. In contrast to $Si_{10}H_{16}$, the low-energy $Si_{10}H_{14}$ structures only contain at most two six-membered Si rings. Interestingly when we used the AM1 method in the CGA we obtained the molecule complex consisting of the structure **5(a)** and a H_2 molecule as the third lowest AM1 energy $Si_{10}H_{16}$ structure.[16] As noted previously, the results in Table 2 indicate that AM1 assigns too high an energy to six-membered Si rings and this may explain why we found the $Si_{10}H_{14}$ global minimum so readily before. It is also worth noting that all structures except **5(a)** and **5(c)** in Figure 5 contain at least one four-membered Si ring and the data in Table 2 suggest that Si_xH_y clusters containing a four-membered Si ring are likely to have higher relative energy

than clusters with five- or six-membered Si rings. This appears to be generally true for the different $Si_{10}H_{14}$ structures although **5(b)** and **5(d)** do contain four-membered Si rings while still being close in energy to **5(c)**. This explains why clusters with surface silyl groups are absent because the remaining Si_9 core would contain more high-energy three- or four-membered Si rings. Another consequence is that in Figure 5 we do not find any $Si_{10}H_{14}$ structures corresponding to an even lower H-passivation, where H_2 is lost, since this would also result in a structure that contains more small Si rings or even a Si atom with dangling bonds. This is also supported by our previous work where we found that the lowest MP2 energy $Si_{10}H_{12}$ clusters have at least two four-membered Si rings.[16]

To determine what level of H-passivation Si_{10} prefers we computed the Gibbs free energy obtained by augmenting the MP2/6-31G* electronic energy with data from a HF/6-31G* vibrational frequency calculation on the optimized structures. The computed Gibbs free energy indicates that the $Si_{10}H_{16}$ 4(a) structure is around 7.8 kcal/mol more stable than the $Si_{10}H_{14}$ **5(a)** structure and a H_2 molecule at 0 K. Not surprisingly, at room temperature this Gibbs free energy difference is reduced appreciably to 2.5 kcal/mol by a translational entropy contribution arising mainly from the H_2 molecule, suggesting that the H_2 and the $Si_{10}H_{14}$ **5(a)** complex are nearly as stable as the $Si_{10}H_{16}$ global minimum structure.

The $Si_{10}H_{14}$ global minimum **5(a)** demonstrates why cluster global optimization techniques, such as the CGA, are useful computational tools. Clearly, structure **5(a)** cannot be readily generated by simply removing two H atoms from the $Si_{10}H_{16}$ global minimum structure **4(a)** and then performing a local geometry optimization. The Si atoms in **4(a)** are arranged as a fragment of the bulk Si lattice with several Si_6 rings, whereas the Si framework in **5(a)** is quite different with mostly Si_5 rings. In our previous CGA on $Si_{10}H_{16}$ we may have correctly found the $Si_{10}H_{14}$ global minimum using the AM1 parameters because as Figure 5 shows the low-energy $Si_{10}H_{14}$ structures generally only contain one six-membered Si ring.[16] The GAM1 parameters from the Si_7H_{14} training set now enable us to confirm more carefully that the $Si_{10}H_{14}$ and $Si_{10}H_{16}$ global minima do have quite different structures.

$Si_{14}H_{20}$. We performed three independent CGA runs each with 9000 local geometry optimizations to search for the global minimum for the $Si_{14}H_{20}$ stoichiometry using the GAM1 parameters obtained from the Si_7H_{14} training set. The 20 lowest energy GAM1 structures **6(a−t)** after locally optimizing at the MP2/lanl2dz level are shown in Figure 6. Two of the CGA runs locate the structure **6(c)** as the lowest GAM1 energy cluster, while the other run locates the structure **6(a)** as the lowest GAM1 energy cluster. Unfortunately the CGA does not succeed in finding the ab initio $Si_{14}H_{20}$ global minimum, which all of our calculations so far suggest to be structure **6(u)** corresponding to a Si_{14} core having a diamond-lattice-like structure fully passivated by 20 H atoms. In our previous CGA using AM1, we found at least 20 $Si_{14}H_{20}$ structures with AM1 energies less than that of **6(u)**[16] but now both the MP2 and GAM1 calculations produce the lowest energy for **6(u)**. We still do not find the diamond-lattice structure **6(u)** among any of the structures obtained by the three CGA runs even though it is another 0.4 kcal/mol lower in GAM1 energy than the twenty **6(a−t)** clusters found by the CGA. One reason finding **6(u)** is so difficult is because the GAM1 energies for the 20 **6(a−t)** clusters have only a 3 kcal/mol spread. The 19 lowest $Si_{14}H_{20}$ structures found in the CGA are also all within 5 kcal/mol of each other at the ab initio level and generally correspond to a fairly similar Si_{13} core structure with a silyl group at different locations. We did obtain **6(h)**, which does not contain any silyl groups and appears to have a Si_{14} core resembling closest the global minimum structure **6(u)**.

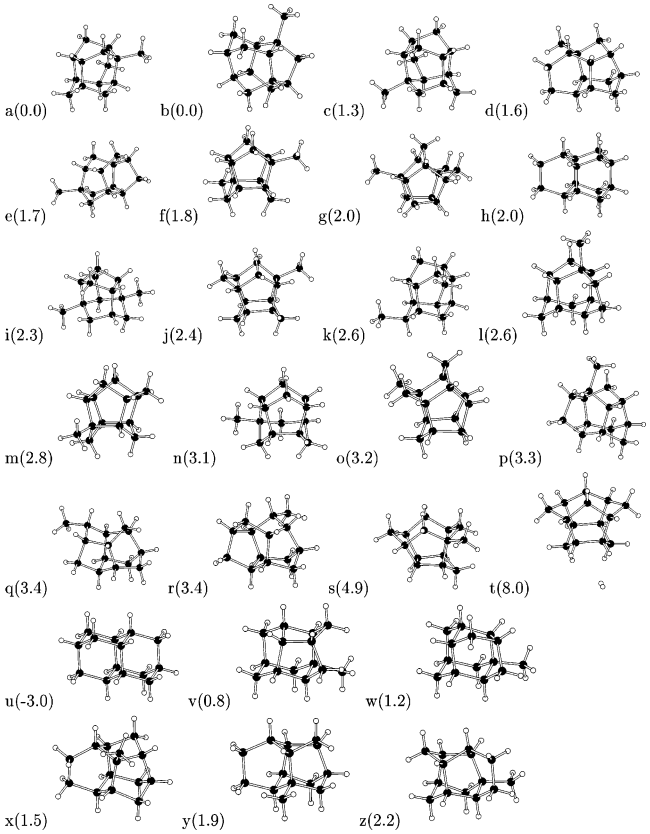

Figure 6. MP2/lanl2dz(d) optimized $Si_{14}H_{20}$ structures. The MP2 relative energies are given in parentheses in kcal/mol. Structures **a−t** were obtained from the CGA while structure **u** is the proposed global minimum at both GAM1 and MP2 levels. Structures **v** and **w** were obtained from the seeded CGA.

To test further whether the diamond-lattice-like structure is the global minimum at the GAM1 level, we ran a seeded CGA where we included structure **6(u)** as one of the starting structures in the initial generation instead of using all randomly fabricated ancestors. The seeded CGA has both advantages and disadvantages when compared against the regular CGA without any seeds in the first population. The seeded GA obviously introduces prejudice into the CGA since it generates low-energy clusters faster than the regular GA simply because from the beginning the seeded CGA runs contain low-energy structures which can be utilized to provide good partial structures to form low-energy offspring. However, we do not find the seeded GA to produce any new $Si_{14}H_{20}$ structures with lower GAM1 energy than the diamond-lattice structure **6(u)**, supporting that the **6(u)** structure is the GAM1 global minimum. The seeded GA also locates the structure **6(c)** as the next lowest GAM1 energy cluster. In addition two new low GAM1 energy structures **6(v)** and **6(w)** which have a very similar Si framework as the MP2 global minimum **6(u)** were located. To explore more possible low-energy cluster structures at the ab initio level, we performed another seeded GA starting with the **6(u)** structure and 20 $Si_{14}H_{20}$ cluster structures we obtained in our previous research.[16] This second seeded CGA located three more low GAM1 energy clusters **6(x−z)** which appear to be higher energy modifications of **6(u)** but are different from the seed structures and the **6(a−**

w) structures. The present results further support that the structure **6(u)** is the global minimum at both the GAM1 and MP2 level.

We notice that many of the low-energy $Si_{14}H_{20}$ clusters again have very similar Si_{13} frameworks but with a silyl group at different surface positions. In contrast, structure **6(u)** contains a distinct Si_{14} framework that cannot as readily be obtained from the mating procedures when either of the two parents has a silyl group. Structure **6(h)** is one of the only structures without a silyl group but it would take a very fortunate cluster cut and mating operation before structure **6(u)** could be generated. A part of the reason that structure **6(u)** may be so difficult to obtain is due to the covalent nature of the Si and H bonds, the global optimization of clusters composed of only one element will always be easier because there will always be some atoms with incomplete bonding. We had a similar problem in the global optimization of the incompletely passivated Si_6H_6 stoichiometry, where we could find fairly easily the optimal Si_6 framework but our mating processes did not readily allow the identification of the best H atom positions.[19] Presently we are investigating whether a mutation operation could be developed that would enable a SiH_2 group to be inserted between or removed from two other neighboring Si atoms.

Interestingly, the highest energy structure **6(t)** shown in Figure 6 corresponds to $Si_{14}H_{20}$ losing a H_2 molecule and is suggestive of possible over-H-passivation. Previously, and obviously unrealistically, we obtained this same **6(t)** structure as the AM1 global minimum of the $Si_{14}H_{20}$ stoichiometry.[16] Thus, although we still do not obtain diamond-lattice-like structure **6(u)** as the lowest energy structure in the CGA, using the GAM1 parameters from the Si_7H_{14} training set does produce a semiempirical method that excels the AM1 method by correctly ranking the **6(u)** as the global minimum in perfect agreement with the ab initio method.

$Si_{14}H_{18}$. To further investigate whether the $Si_{14}H_{18}$ cluster in the above **6(t)** structure is also the GAM1 and/or MP2 global minimum cluster with $Si_{14}H_{18}$ stoichiometry, we have performed three independent CGA runs each with 9000 local geometry optimizations to search for the global minimum with the $Si_{14}H_{18}$ stoichiometry. All three CGA runs locate the same $Si_{14}H_{18}$ global minimum after 1290, 6420, and 1800 local geometry optimizations. The resulting 20 lowest GAM1 energy $Si_{14}H_{18}$ clusters after locally optimizing at the MP2 level are shown in Figure 7. As expected the $Si_{14}H_{18}$ GAM1 global minimum, structure **7(a)**, is the same $Si_{14}H_{18}$ cluster shown in the **6(t)** structure. Since **7(a)** contains only three six-membered Si rings our previous CGA on $Si_{14}H_{20}$ with AM1[16] and the present CGA with the GAM1 parameters appear to have little difficulty in finding this global minimum. Indeed, we can now understand our previous result since the present work shows that the AM1 calculations are assigning too high a relative energy to six-membered Si rings and the $Si_{14}H_{18}$ in **6(t)** (or **7(a)**) has fewer six-membered rings than the other lower energy $Si_{14}H_{20}$ structures. The fact that **7(a)** is also the lowest MP2 energy cluster further justifies the transferability of the GAM1 parameters obtained by using a Si_7H_{14} training set. Unlike the **6(u)** diamond-lattice structure where all the six-membered Si rings adopt the chair conformation, the three six-membered Si atom rings in structure **7(a)** all have the boat conformation. We expect the H atoms at the "flagpole" positions on the Si_6 rings to repel each other since they are separated by only ≈2.9 Å. This may explain why the structures **7(b)** and **7(c)** are less than 1 kcal/mol higher in energy than **7(a)** since **7(b)** and **7(c)** lose two flagpole H atoms and its underlying Si to give a silyl group that binds at different positions on the remaining Si_{13} framework. Besides structures **7(b)** and **7(c)**, many other low MP2 energy clusters such as structures **7(d−h)** have Si frameworks similar to the **7(a)** structure and as a consequence are within a small 2 kcal/mol energy range. The energy range for the 20 lowest energy $Si_{14}H_{18}$ clusters is only 5.3 kcal/mol and is significantly narrower than the 19.9 kcal/mol determined for $Si_{10}H_{14}$. We think this is because all Si atoms in $Si_{14}H_{18}$ are able to remain tetrahedrally coordinated without requiring any three- or four-membered Si rings to be formed.

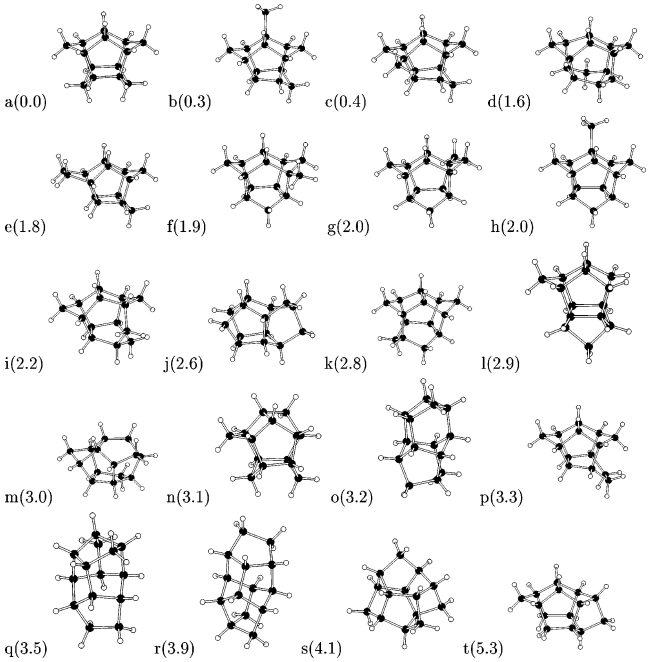

Figure 7. MP2/lanl2dz(d) optimized $Si_{14}H_{18}$ structures. The MP2 relative energies are given in parentheses in kcal/mol.

The inclusion of the HF/3-21G ZPE calculation suggests that the Gibbs energy of the $Si_{14}H_{20}$ **6(u)** diamond-lattice-like structure is 7.6 kcal/mol lower than the total Gibbs energy of the $Si_{14}H_{18}$ **7(a)** structure and a H_2 molecule at 0 K. However, the entropy contribution from the translational mode of the H_2 molecule causes the total Gibbs free energy of a H_2 molecule and a $Si_{14}H_{18}$ **7(a)** cluster to be only 2.7 kcal/mol higher than that of the diamond-lattice-like $Si_{14}H_{20}$ global minimum cluster at room temperature.

The CGA with the Si_7H_{14} GAM1 parameters find a global minimum **7(a)** for $Si_{14}H_{18}$ that is consistent with our earlier CGA results on $Si_{14}H_{20}$ using AM1. The $Si_{14}H_{18}$ global minimum cannot be simply obtained by removing two H atoms from the $Si_{14}H_{20}$ global minimum **6(u)** but it does contain only three six-membered Si rings enabling both AM1 and GAM1 to locate **7(a)**. However, since the Si_7H_{14} GAM1 parameters produce $Si_{14}H_{20}$ and $Si_{14}H_{18}$ global minima and low-energy structures better matching the MP2 rankings we have greater confidence in the present results.

4. Conclusion

We have applied a parametrization genetic algorithm (PGA) to determine the GAM1 parameters using a Si_7H_{14} training set consisting of 14 different structures locally optimized at the MP2/6-31G* level. The resulting GAM1 method reproduces the Si_7H_{14} MP2/6-31G* relative energies and geometries in better agreement than the original AM1 method. The GAM1 parameters appear to correct for the too high relative energy calculated by AM1 for structures containing six-membered Si rings.

Rather than perform the coupled PGA and cluster genetic algorithm (CGA) to find the global minimum structure for large clusters we have investigated the transferability of the GAM1 parameters derived from a Si_7H_{14} training set to larger clusters. We first evaluated the GAM1 optimized energies of the clusters with various stoichiometries ($Si_{10}H_y$, $y = 4$, 8, 12, 16, 20, and $Si_{14}H_{20}$) we located in previous research work.[16] Our results show that the GAM1 and MP2 relative energies and energy rankings match well for the $Si_{10}H_{16}$, $Si_{10}H_{20}$, and $Si_{14}H_{20}$ stoichiometries which have a similar level of passivation as the Si_7H_{14} stoichiometry.

To further illustrate the transferability of the GAM1 parameters for larger clusters, we have globally optimized the $Si_{10}H_{14}$, $Si_{10}H_{16}$, $Si_{14}H_{18}$, and $Si_{14}H_{20}$ clusters using the Si_7H_{14} GAM1 parameters to evaluate the cluster energies. We find the GAM1 and MP2 energy rankings match well for each of the 4 above stoichiometries and the GAM1 global minimum clusters also have the lowest MP2 energies. Unlike for the AM1 calculations, we find the diamond-lattice-like $Si_{10}H_{16}$ and $Si_{14}H_{20}$ structures to have the lowest GAM1 and MP2 energies. These results further confirm that the $Si_{10}H_{16}$ and $Si_{14}H_{20}$ clusters prefer diamond-lattice structures at 0 K. However, vibrational frequency calculations show that the total Gibbs free energy of the $Si_{10}H_{14}$ or $Si_{14}H_{18}$ global minimum and a H_2 molecule is close to that of the diamond-lattice $Si_{10}H_{16}$ or $Si_{14}H_{20}$ cluster respectively at room temperature.

Finally, the ability to transfer GAM1 parameters obtained from a Si_7H_{14} training set to larger well-passivated Si_xH_y clusters should enable us to develop a fast global optimization strategy for larger Si_xH_y clusters at the ab initio level providing the GAM1 parameters are obtained from a training set built from a specific stoichiometry with a comparable level of passivation.

Acknowledgment. We are grateful for the generous use of the IBM SP system at the Maui High Performance Computer Center and the SP system donated to the University of Hawaii by IBM.

References and Notes

(1) Sari, L.; McCarthy, M. C.; Schaefer, H. F.; Thaddeus, P. *J. Am. Chem. Soc.* **2003**, *125*, 11409.

(2) Chambreau, S. D.; Wang, L. M.; Zhang, J. S. *J. Phys. Chem. A* **2002**, *106*, 5081.

(3) Katzer, G.; Ernst, M. C.; Sax, A. F.; Kalcher, J. *J. Phys. Chem. A* **1997**, *101*, 3942.

(4) Onida, G.; Andreoni, W. *Chem. Phys. Lett.* **1995**, *243*, 183.

(5) Miyazaki, T.; Uda, T.; Stich, I.; Terakura, K. *Surf. Sci.* **1997**, *377*, 1046.

(6) Miyazaki, T.; Uda, T.; Stich, I.; Terakura, K. *Chem. Phys. Lett.* **1996**, *261*, 346.

(7) Miyazaki T.; Uda T.; Stich I.; Terakura K. *Chem. Phys. Lett.* **1998**, *284*, 12.

(8) Meleshko, V.; Morokov, Y.; Schweigert, V. *Chem. Phys. Lett.* **1999**, *300*, 118.

(9) Meleshko, V. P.; Morokov, Y. N.; Schweigert, V. A. *J. Struct. Chem.* **1999**, *40*, 10.

(10) Meleshko, V. P.; Morokov, Y. N.; Schweigert, V. A. *J. Struct. Chem.* **1999**, *40*, 503.

(11) Swihart, M. T.; Girshick, S. L. *Chem. Phys. Lett.* **1999**, *307*, 527.

(12) Judson R. In *Reviews in Computational Chemistry*; Lipkowitz, K. B., Boyd, D. B., Eds.; VCH: New York, 1999; Vol. 10, p 1.

(13) Johnston, R. L. *Dalton Trans.* **2003**, 4193.

(14) Deaven, D. M.; Ho, K. M. *Phys. Rev. Lett.* **1995**, *75*, 288.

(15) Hartke, B. *J. Comput. Chem.* **1999**, *20*, 1752.

(16) Ge, Y.; Head, J. D. *J. Phys. Chem. B* **2002**, *106*, 6997.

(17) Dewar, M. J. S.; Zoebisch, E. G.; Healy, E. F.; Stewart, J. J. P. *J. Am. Chem. Soc.* **1985**, *107*, 3902.

(18) Tsai, C. J.; Jordan, K. D. *J. Phys. Chem.* **1993**, *97*, 11227.

(19) Ge, Y.; Head, J. D. *Int. J. Quantum Chem.* **2003**, *95*, 617.

(20) Hartke, B. *Chem. Phys. Lett.* **1996**, *258*, 144.

(21) Hartke, B. *Theor. Chem. Acc.* **1998**, *99*, 241.

(22) Dewar, M. J. S.; Jie, C. *Organometallics* **1987**, *6*, 1486.

(23) GAMESS, The General Atomic and Molecular Electronic Structure System; Schmidt, M. W.; Baldridge, K. K.; Boatz, J. A.; Elbert, S. T.; Gordon, M. S.; Jensen, J. H.; Koseki, S.; Matsunaga, N.; Nguyen, K. A.; Su, S.; Windus, T. L.; Dupuis, M.; Montgomery, J. A., Jr. *J. Comput. Chem.* **1993**, *14*, 1347.

(24) Møller, C.; Plesset, M. S. *Phys. Rev.* **1934**, *46*, 618.

(25) Francl, M. M.; Pietro, W. J.; Hehre, W. J.; Binkley, J. S.; Gordon, M. S.; Defrees, D. J.; Pople, J. A. *J. Chem. Phys.* **1982**, *77*, 3654.

(26) Hehre, W. J.; Ditchfield, R.; Pople, J. A. *J. Chem. Phys.* **1972**, *56*, 2257.

(27) Rossi, I.; Truhlar, D. G. *Chem. Phys. Lett.* **1995**, *233*, 231.

(28) Wadt, W. R.; Hay, P. J. *J. Chem. Phys.* **1985**, *82*, 284.

(29) Rohlfing, C. M.; Raghavachari, K. *Chem. Phys. Lett.* **1990**, *167*, 559.

(30) Dunning, T. H., Jr.; Hay, P. J. In *Modern Theoretical Chemistry*; Schaefer, H. F., III, Ed.; Plenum: New York, 1977; Vol. 3, p 1.

(31) Krüger, T.; Sax, A. F. *J. Comput. Chem.* **2001**, *22*, 151.

(32) Scott, A. P.; Radom, L. *J. Phys. Chem.* **1996**, *100*, 16502.